

EVALUATION OF DIFFERENT PERFORATION PATTERNS FOR LAMINATE-INTEGRATED HEATING FOILS IN WIND TURBINE ROTOR BLADES

Jan E. Semar¹, David May² and Peter Mitschang³

¹Institut für Verbundwerkstoffe GmbH, Impregnation & Preform Technologies,
Erwin-Schrödinger-Str. 58, Germany

Email: JanEric.Semar@ivw.uni-kl.de, Web Page: <http://www.ivw.uni-kl.de>

²Institut für Verbundwerkstoffe GmbH, Impregnation & Preform Technologies,
Erwin-Schrödinger-Str. 58, Germany

Email: David.May@ivw.uni-kl.de, Web Page: <http://www.ivw.uni-kl.de>

³Institut für Verbundwerkstoffe GmbH, Manufacturing Science,
Erwin-Schrödinger-Str. 58, Germany

Email: Peter.Mitschang@ivw.uni-kl.de, Web Page: <http://www.ivw.uni-kl.de>

Keywords: wind energy, heating foil, perforation, de-icing, anti-icing

Abstract

Icing of rotor blades is a limiting factor for the energy production of wind turbines. Laminate-integrated heating foils can be used to decrease icing related power loss. To avoid damages due to environmental conditions, the heating foil must not be placed on the blades' outside but as close as possible to it in the laminate to ensure maximum heating efficiency. However, as modern rotor blades are manufactured by vacuum assisted resin infusion, liquid resin has to flow through the heating foil during impregnation, which requires a suitable perforation. To achieve fast infusion and efficient heating at the same time, the influence of perforation diameter, degree of coverage and perforation arrangement on through-the-thickness permeability, heating capacity, temperature distribution and interlaminar shear strength were investigated. It was found that the relative perforation area is the dominant factor, especially for permeability, heating power and shear strength. The perforation diameter had small influence while the perforation arrangement was only slightly relevant for temperature distribution and permeability. Based on these results guidelines for a suitable perforation design have been developed.

1. Introduction

Icing is a serious threat for wind energy turbines in cold climates. It can damage the turbines through imbalance, endanger people, animals, goods and properties through jettisoned ice chunks and can lead to an annual power loss of up to 50% [1, 2]. Several approaches exist to avoid the formation of ice on rotor blades (anti-icing) or to remove it (de-icing) [3]. In the research project "HyRoS" [4], a new system for anti-icing as well as de-icing is investigated: A heating foil integrated into the composite of the rotor blade, as close to the aerodynamic surface as possible. By this, the reaction times of the heating control system can be minimized and the heating can be concentrated on the outer layers of the composite without exposing the heating foil to harmful environmental conditions like UV-light or rain erosion. Furthermore, the heating foil can be divided into several sectors with different power settings, matching the locally required heat flux. This leads to maximum energy efficiency.

However, as today's rotor blades are usually manufactured by vacuum assisted through-the-thickness impregnation of dry glass fiber textiles with epoxy or polyester resins, the heating foil poses a barrier to the impregnation and hence has to be perforated. The influence of three different perforation

parameters on heating power and temperature distribution, permeability and shear strength has been evaluated.

2. Materials and Methods

2.1. Materials

As heating foil the product “FlexiWarm” from the company “K.L. Kaschier- und Laminier GmbH” has been used. It is conductive by itself, so that no heating wires are required. Hence, damages to the foil, like holes or cuts, reduce the available area for the electrical current and therefore the conductivity, but do not lead to complete failure. Power supply is provided by wires at the edge of the foil. The foil’s total thickness is around 0.4 mm. For the shear strength tests, the heating foil was integrated into a glass fiber reinforced composite (GFRP). The used textile was the biaxial non-crimped fabric “SAERTEX X-E-812 g/m²” As resin for the impregnation, the epoxy “Hexion RIMR 135” with the hardener “Hexion RIMH 137” has been selected.

2.2 Perforation

As result of pilot experiments, only circular perforations with material removal have been further investigated. Non-circular perforations, e.g. elliptically or star-shaped, could be used to influence the drapeability of the foil but also reduce the reproducibility of the experiments.

For the experiments, three perforation parameters have been varied:

1. The perforation diameter
2. The degree of coverage (*DoC*) of the heating foil, defined as:

$$DoC = \frac{(A_{np} - A_h)}{A_{np}} = \frac{A_p}{A_{np}} \quad (1)$$

With the area of the non-perforated foil A_{np} , the area of the perforation holes A_h and the foil’s area after perforation A_p

3. The perforation arrangement, either as triangular or quadratic pattern (see Figure 1).

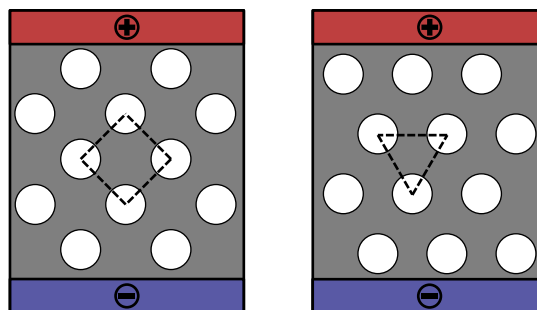


Figure 1. Symbolic depiction of perforation arrangements. Left: quadratic, right: triangular.

For serial production of perforated heating foils, the perforation can be created by punching machines. However, as there is a separate punching tool necessary for each perforation pattern, this method is not suitable for experiments. Instead, the perforation has been manufactured on a CNC-cutter. This sets the lower limit of the examined perforation diameter to 2.5 mm, as it was not possible to reliably cut

out smaller holes. Puncturing the foil with sewing needles without material removal did not result in an acceptable permeability, as the holes reclosed during impregnation and no sufficient impregnation was possible.

Design of experiment methods have been employed to create optimized test coverage and a full-factorial experiment plan of the type 2^3 has been selected. The values can be seen in Table 1. As the manufacturing of the perforation on a cutter proved to be very time consuming, only one repetition per experiment could have been performed.

Table 1. Values of the perforation parameters for a full-factorial experiment plan of the type 2^3

Parameter	Value A	Value B
Perforation diameter	2.5 mm	4.0 mm
Degree of coverage	75%	95%
Perforation arrangement	Triangular	Quadratic

2.3 Experimental setup

For the experiments, heating foils with a length of 300 mm, a width of 170 mm and a distance between the electrodes of 130 mm have been used (see Figure 2). The electrical resistance R of the foils has been measured before and after perforation and the expected increase has been monitored.

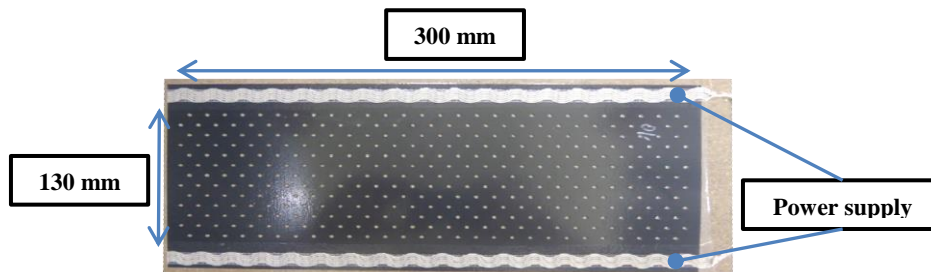


Figure 2. Exemplary depiction of a perforated heating foil.

In the next step, the influence of the perforation on the heating behavior of the heating foils was investigated. A vacuum build-up was used to fix the film on a thick wood plate to ensure even heat transfer and avoid hotspots by lifting the film off the substrate (see Figure 3). The heating foils were heated one after another with direct current I . For safety reasons, the voltage U has been limited to safety extra-low voltage (SELV). The heating power can be calculated with the well-known Ohm's Law (2) and the formula for the electrical power P (3).

$$U = R * I \quad (2)$$

$$P = U * I = R * I^2 = \frac{U^2}{R} \quad (3)$$

There was no current limitation other than the resistance of the heating foil itself. Using a thermal camera, the average, maximum and minimum temperatures of each film were determined after a heating time of ten minutes. A thermocouple at the top of the reference foil was used to calibrate the thermal imaging camera with regard to the emission coefficient of the heating foil.

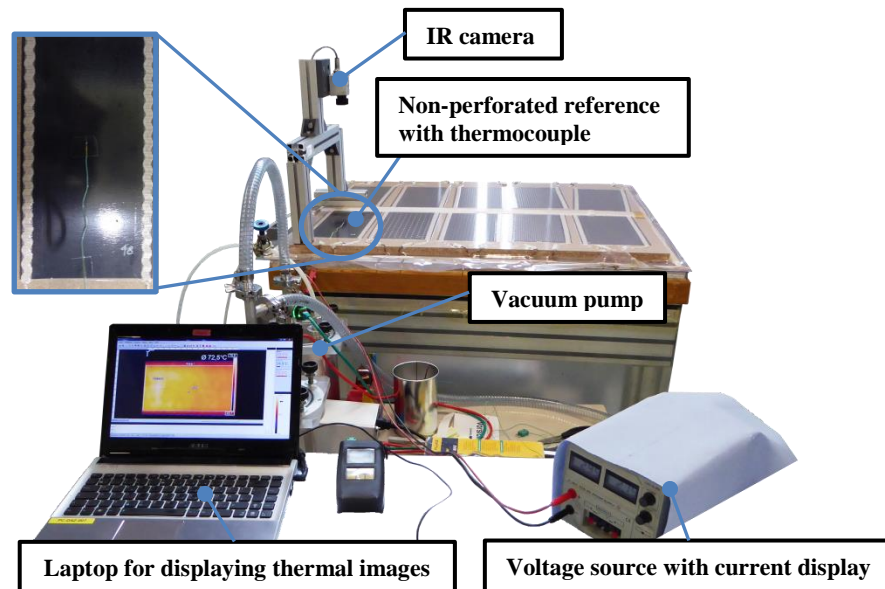


Figure 3. Experimental setup for the heating distribution assessment via infrared camera

In an independent test, the influence of the heating foil on the through-the thickness permeability of a textile preform has been examined. The measurement has been done with the “HyKoPerm” system, as described in [5]. Therefore, elliptical heating foil specimens without electrodes and axis lengths of 196 mm and 156 mm have been placed in the middle of a stack of eight textile layers and were compacted to a fiber volume content of 50%. Injection was done with a pressure difference of 0.5 bar.

The rectangular heating foils were subsequently embedded into a glass fiber reinforced composite by vacuum infusion, to create specimens for tensile shear tests. To achieve maximum stiffness and provoke shear failure in the heating foil, 20 layers of the textile were used, with the foil in the middle of the stack. Since an increase in the electrical resistance of the heating foil due to the impregnation could be observed in previous experiments, the electrical resistance was examined again after impregnation.

To create a defined overlap length for the shear tests, two stripes of polyimide adhesive tape were glued to the heating foils, parallel to the power supply wires (see Figure 4). This proved to be more reproducible than an exact positioning of the incisions, which were required to ensure that the test force is introduced into the heating foil as shear force. The epoxy resin adheres very poorly to the tape, so that no relevant force transmission occurred in this area. In order to investigate the influence of the perforation pattern, samples with a sufficient size must be tested. If the sample is smaller than the unit cell of the pattern, actual DoC in the sample deviates from its theoretical value. Therefore, the distance between the adhesive strips was selected as 80 mm, with a specimen width of 25 mm. The samples have then been inserted into a tensile testing machine and the stress at failure as well as the failure mode has been observed.

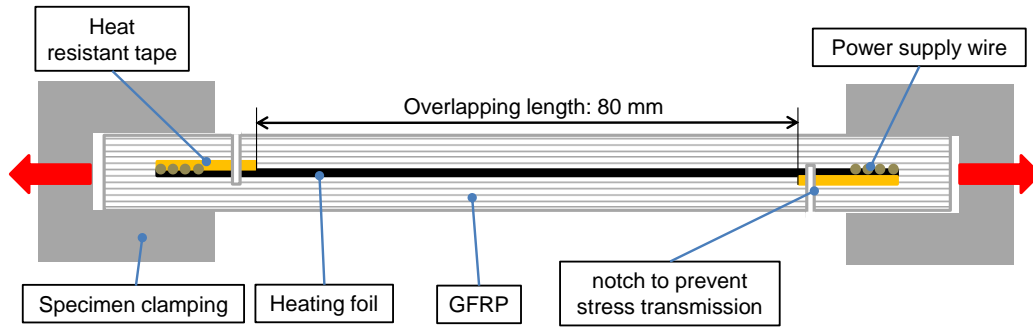


Figure 4. Schematic test setup for tensile shear test, non-scaled side view

3. Results

3.1 Influence of the perforation on the through-the-thickness permeability

The heating foil induced permeability reduction, compared to a reference stack without heating foil, was in the range of 16 % to 75 % and therefore far outside of the standard deviation of the five reference measurements (see Figure 5). A low degree of coverage resulted in a higher permeability than a high *DoC*. It seems that a smaller perforation diameter has a slight permeability increasing effect, although this could not be proven beyond doubt in the statistical evaluation. The same applies for a triangular arrangement. Further investigation will follow.

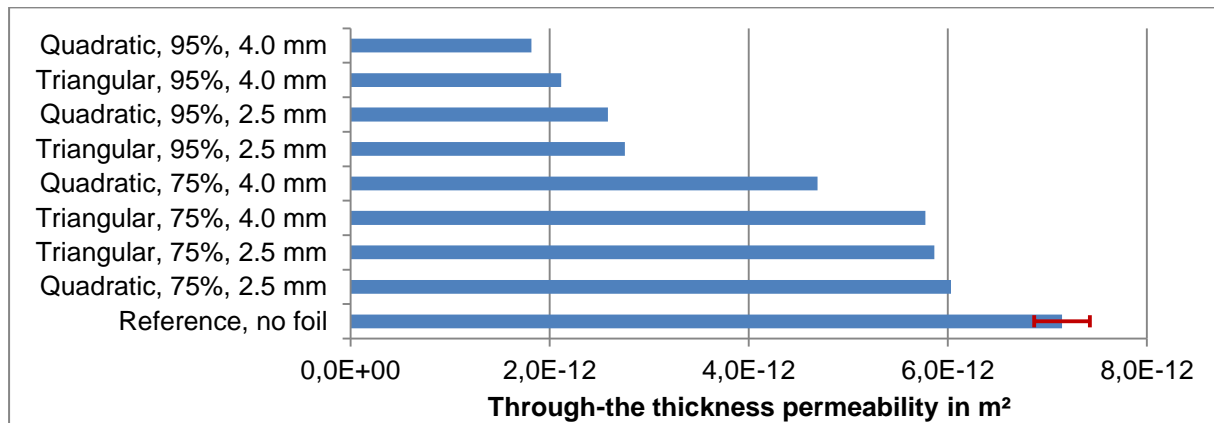


Figure 5. Heating foil influence on permeability of textile preforms, reference with standard deviation

3.2 Influence of the perforation on the heating foil's resistance

A major concern was the perforation's influence on the resistance of the heating foil, and therefore its heating power for a given voltage supply. The electrical resistance of the specimens has been measured before and after perforation, the results can be seen in Table 2. The increase in resistance was only affected by the degree of coverage. A *DoC* of 95% resulted in a mean resistance increase of 13% and a *DoC* 75% increased the resistance by 76%. The perforation arrangement and the perforation diameter had no statistically significant effect.

Table 2. Electrical resistance of heating foils before and after perforation and after impregnation

Perforation parameters			Resistance before perforation	Resistance after perforation	Resistance after impregnation
Perf. diameter	Degree of coverage	Perf. arrangement			
	Non-perforated reference		13.0 Ω	---	16.0 Ω
2.5 mm	75%	Triangular	13.5 Ω	25.5 Ω	31.0 Ω
2.5 mm	75%	Quadratic	13.0 Ω	22.7 Ω	27.8 Ω
2.5 mm	95%	Triangular	13.2 Ω	14.8 Ω	17.7 Ω
2.5 mm	95%	Quadratic	13.2 Ω	15.0 Ω	18.4 Ω
4.0 mm	75%	Triangular	13.3 Ω	22.7 Ω	27.3 Ω
4.0 mm	75%	Quadratic	13.6 Ω	22.9 Ω	27.9 Ω
4.0 mm	95%	Triangular	13.1 Ω	14.9 Ω	17.3 Ω
4.0 mm	95%	Quadratic	13.3 Ω	14.9 Ω	17.5 Ω

Table 2 also shows the resistance after impregnation. All foils showed a similar resistance increase of around 21%. The increased heating foil resistance after impregnation might be a result of the deformation of the foil, as it follows the textile's compaction and nesting. This stretches the foil and reduces its cross sectional area. This would explain the almost constant percentage increase of the resistance for all perforations and the non-perforated reference. Further investigation is necessary for this matter.

3.3 Influence of the perforation on the heat distribution

The heat distribution of the heating foils has been assessed by thermographic imaging and comparing the minimum and maximum temperature in the evaluation area. The aim is to achieve a homogeneous temperature distribution in order to avoid ice build-up at cold spots on the rotor blade's surface. The temperature distribution is more relevant, the closer the heating foil is positioned to the surface, as the composite has a homogenizing effect. Low *DoC* and especially small perforation diameters resulted in a more homogeneous temperature distribution. An example is given in Figure 6. The figure shows both perforations with a *DoC* of 75% and a quadratic pattern, once with 4.0 mm perforation diameter, once with 2.5 mm. As result of the smaller holes, this in turn means a higher number to reach the same *DoC*, no cold spots can be observed anymore. It also seems that a triangular pattern results in a better homogeneity than a quadratic one, however this effect is small and the gathered data is not sufficient for a final evaluation.

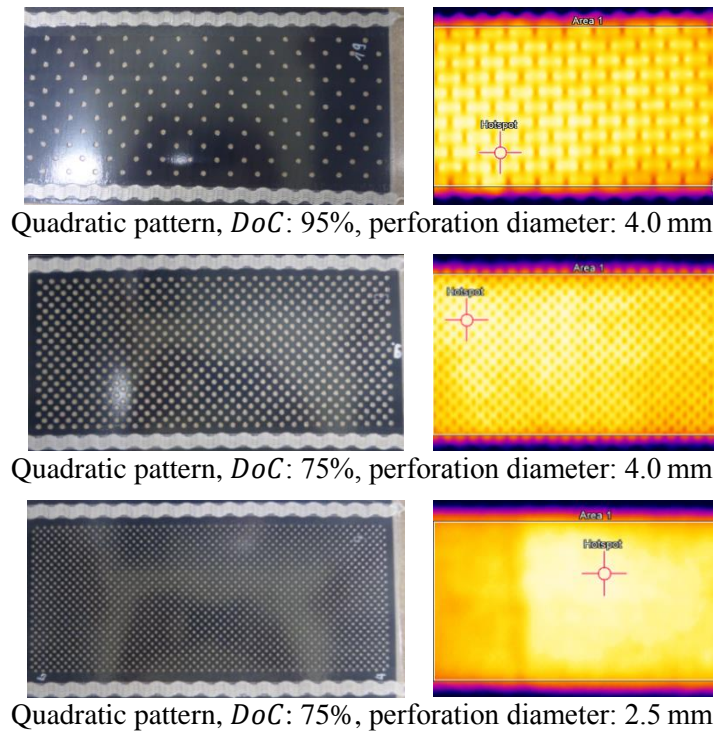


Figure 6. Heat distribution depending on perforation parameters. Left: visible light, Right: infrared

3.4 Influence of the perforation on the shear strength

The tensile shear test has been used to quantify the expected loss in shear strength of a GFRP laminate as result of the introduction of the heating foil. However, the opposite has been observed.

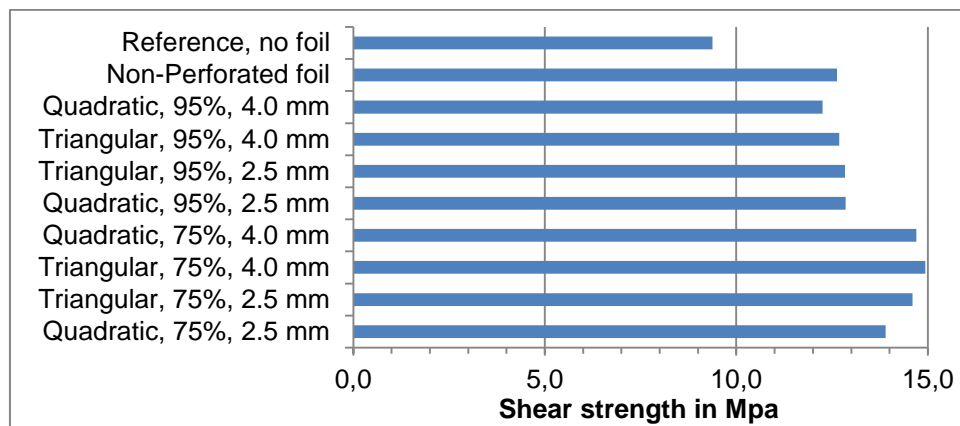


Figure 7. Shear strength of the different foils, the reference is the composite without foil

Figure 7 shows that the degree of coverage has a relevant influence on the breaking shear stress. The lower the *DoC*, the better the joint strength. On the other hand, a breaking shear stress of more than 12 MPa is also achieved with the non-perforated heating foil. An influence of pattern or diameter was not observed. Remarkable are the significantly lower breaking shear stresses in the reference tests without foil. Here, an average of only 9.4 MPa is achieved. The reason therefore is most likely the difference in the failure mode. The specimens with foil failed at once, with a loud crack, as the

adhesion between the heating foil and the composite is so strong that failure occurred inside the heating foil and its remains stay on both parts of the specimen. The reference specimens showed a gradually failure with crack propagation in several layers of the laminate (see Figure 8).

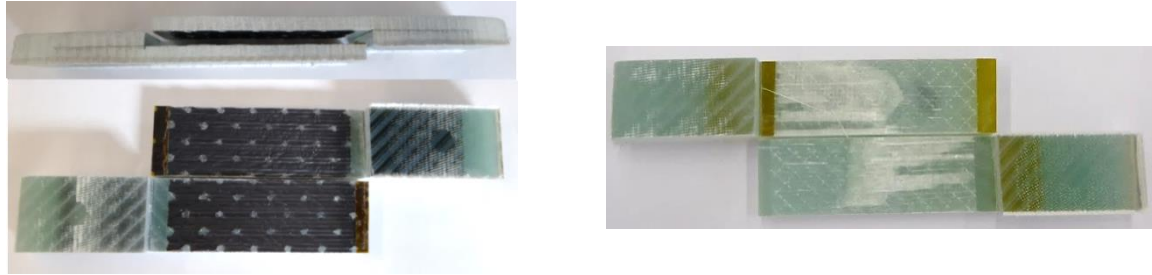


Figure 8. Fracture surface of shear test specimens. Left: with heating foil, Right: reference without

4. Conclusions

The influence of three perforation parameters for laminate-integrated heating foils with respect to the foil's resistance (and therefore power), the homogeneity of its heating, its influence on a laminate's shear strength and permeability have been evaluated. The largest influence has been observed for the degree of coverage. While the shear strength and permeability are increased by smaller *DoC*, heating power is decreased. Therefore, a suitable compromise must be found for each application, i.e. using higher *DoC* in blade areas with higher heat requirements. Lower perforation diameters increase the homogeneity of the temperature distribution and probably the permeability, so it is preferable to choose them as small as possible. In the conducted experiments, a lower limit could not be determined due to the technically feasible minimum perforation diameter. However, it is expected that with diameters in the same magnitude as the film thickness of 0.4 mm, the assumption of flow behavior no longer applies and permeability declines. For the two tested perforation arrangements, no significant influence regarding all results has been observed. While the triangular pattern might possibly be slightly advantageous regarding temperature distribution and permeability, the acquired data is not sufficient to prove this beyond doubt.

Acknowledgments

This work is part of the "HyRoS" project, funded by the German Federal Ministry for Economic Affairs and Energy, project funding reference number: 0325937G. We would like to thank all of our project partners for their support.

References

- [1] B. Tammelin *et al.*, "Wind Energy Production in Cold Climate (WECO)," 1998.
- [2] L. Battisti, *Wind Turbines in Cold Climates: Icing Impacts and Mitigation Systems*. Cham: Springer International Publishing, 2014, ISBN: 978-3-319-05190-1.
- [3] O. Parent and A. Ilinca, "Anti-icing and de-icing techniques for wind turbines: Critical review," *Cold Regions Science and Technology*, vol. 65, no. 1, pp. 88–96, 2011.
- [4] [Online] Available: <http://www.hyros-projekt.de/>.
- [5] D. May and P. Mitschang, "Measurement system for on-line compaction monitoring of textile reaction to out-of-plane impregnation," *Advanced Composites Letters*, vol. 23, pp. 32–36, 2014.